

Optical selection rules in superlattices in the envelope-function approximation

P. Voisin, G. Bastard, and M. Voos

Groupe de Physique des Solides de l'Ecole Normale Supérieure, Laboratoire associé au Centre National de la Recherche Scientifique, 24 rue Lhomond, F-75005 Paris, France.

(Received 4 February 1983; revised manuscript received 22 April 1983)

We show that the symmetry properties of the Bloch envelope functions in a superlattice influence considerably the absorption and emission line shapes associated with interband transitions. Absolute values of the absorption coefficients in superlattices are also discussed.

I. INTRODUCTION

Considerable attention has been devoted to the artificial superlattices which can be achieved by molecular-beam epitaxy or metal organic chemical vapor deposition. Up to now, most of the theoretical works¹⁻⁷ have been devoted to calculations of the dispersion relations along the growth axis, but the properties of the superlattice wave functions have been scarcely studied.⁸ They are, however, of major relevance when evaluating the strength and the shape of the absorption and recombination spectra. Assuming perfect lattice matching between host materials, a superlattice crystal displays two periodicities: the natural (d_0) and the artificial (d). Usually, one deals with $d \gg d_0$. The superlattice electronic states have been described either by the tight-binding approach^{1-3,5} or within the framework of the envelope-function approximation.^{4,6,7} The former scheme focuses the attention on atomlike properties (i.e., at the d_0 scale) and builds the superlattice states from host *atomic* site to host atomic site. The latter scheme takes the natural periodicity d_0 into account by means of an effective-mass approximation (eventually multiband) whereas the superperiodicity d acts upon the envelope functions which are slowly varying at the scale of d_0 . The tight-binding calculations are exact in essence but to be accurate they require quite elaborate computational efforts that they are ill suited for actual layer thicknesses (i.e., $d \gg d_0$). In the envelope-function scheme, some microscopic (i.e., at the scale of d_0) information is lost. In particular, the details of interfaces between two consecutive layers and the exact chemical nature of actual host layers (e.g., which are the chemical elements of the two terminating planes of a given layer) are left undefined. In this coarse-grained description, which is reasonable only for sufficiently *thick* host layers, each layer is an effective medium of which only some gaps and interband-matrix element are known. The electron dynamics in the superlattice is described by the envelope functions which are eigenstates of an effective (eventually multiband) Hamiltonian. Again, the only *microscopic* information which has survived in the envelope-function scheme is embodied into a few parameters (in practice, Γ gaps, Γ spin-orbit coupling, and Kane matrix element) which are known from experiments on bulk materials. Despite its apparent crudeness, the envelope-function approximation is in excellent agreement with experiments

[for both the GaAs-Ga(Al)As and InAs-GaSb systems]. This is not very surprising as long as the experiments have been performed on crystals with $d \gg d_0$ for which the interface planes represent a relatively minor detail compared with the "bulk" of each host layers. An important consequence of the smearing out of the atomlike details in the envelope-function scheme is the symmetry property of the superlattice potentials. The superlattice potentials which enter into the effective Hamiltonian governing the envelope functions are even with respect to the centers of the slices of both host materials. In this paper we exploit this property to derive a parity selection for the interband optical transitions (Sec. II). In Sec. III we present an analytical calculation of the interband-matrix element based on a linear combination of atomic orbitals (LCAO) expansion of the *envelope* functions associated with the conduction and valence subbands. The property found in Sec. II is recovered and its influence on the absorption and emission spectra is discussed in Sec. IV.

II. SYMMETRY PROPERTIES OF THE SUPERLATTICE ENVELOPE FUNCTIONS

We consider a binary superlattice (SL) obtained by alternatively stacking layers of *A* material (thickness L_A) and layers of *B* material (thickness L_B). Two cases may be encountered.

(1) Either the same layers (for example, the *A* layers) are quantum wells (QW) for both conduction and valence states (Fig. 1). This situation, so-called "type-I" SL, is met in the GaAs/Al_xGa_{1-x}As system. In this case, the corresponding wave functions are mostly localized in the *A* layers.

(2) Or the quantum wells for conduction (valence) states exist in the *A* (*B*) layers (Fig. 1). This case, referred to as "type-II" SL, is that of the InAs-GaSb system.

In the following, we restrict ourselves to the envelope-function description of the superlattice states.^{4,6,7} The basic assumptions are the following:

(a) The *A* and *B* materials are assumed to be perfectly lattice-matched.

(b) We are primarily dealing with III-V- and II-VI-compound direct-gap materials. Since we want to calculate superlattice states which are close enough from the hosts Γ points, we assume that only the usual $\Gamma_6, \Gamma_7, \Gamma_8$ host-band edges significantly contribute to the superlattice

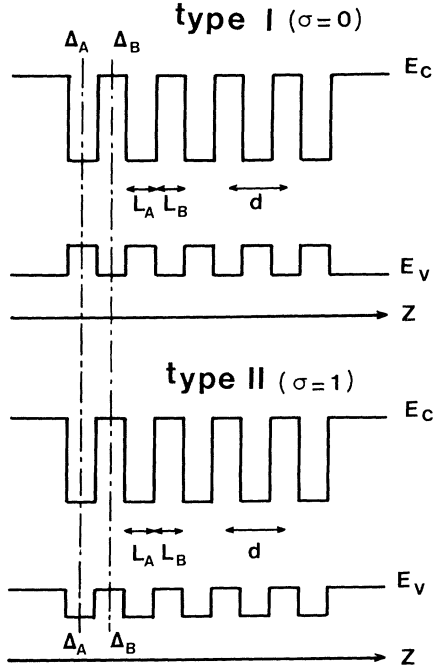


FIG. 1. Modulation of the host-band edges along the growth axis for type-I and type-II SL's.

wave function.

(c) The Γ -point—periodic parts of the hosts Bloch functions u_ν ($1 \leq \nu \leq 8$) are assumed to be identical in A and B layers.

(d) Any inversion-asymmetry effect associated with the zinc-blende lattice is neglected. This quasi-Ge model is known to work very well for the cubic III-V and II-VI compounds as far as Γ -like states are involved.

Then the superlattice wave functions are written as

$$\psi(\vec{r}) = \sum_{\nu=1}^8 u_\nu(\vec{r}) F_\nu(\vec{r}),$$

where the superlattice envelope functions $F_\nu(\vec{r})$, slowly varying at the scale of d_0 , are the solutions of an 8×8 effective Hamiltonian obtained by replacing k_z in the bulk quasi-Ge $\vec{k} \cdot \vec{p}$ Hamiltonian by the operator $-i\hbar \partial / \partial z$ for the kinetic energy and adding a superlattice potential energy term $V_{\nu\nu}(z)$ which is diagonal in ν and represents the jump of the ν th band edge when going from the A material to the B material if flat band conditions prevail. Any envelope function F_ν , $1 < \nu < 8$, is solution of a 1×1 effective Hamiltonian H_ν obtained by projecting the 8×8 effective Hamiltonian onto the ν th edge. H_ν only contains even powers of $\partial / \partial z$, as can be easily deduced from Ref. 6.

Any microscopic details as those occurring at the interfaces (chemical nature of the terminating planes, interface bond lengths, etc.) are washed out in the envelope-function scheme. Such a scheme makes sense for thick host layers ($d \gg d_0$), the actual situation, and is, in fact, in remarkable agreement with experiments (both for the energies and the parity selection rules in GaAs-Ga(Al)As QW's or for the subband energies in InAs-GaSb superlattices). The absence of layer-edge microscopic details has an important consequence on the symmetry properties of the functions F_ν . Indeed consider two consecutive A, B layers. Let O_A, O_B be the centers of the A, B layers and Δ_A, Δ_B the axis bisecting the A, B segments. The product $R_B R_A$ of the two reflections R_A and R_B with respect to Δ_A and Δ_B , respectively, is equal to a transition τ_d of the SL period $d = L_A + L_B$. R_A, R_B and τ_d commute with the effective Hamiltonian H_ν , but not with each other. In fact, we have $[R_A, \tau_d] = R_B(\tau_d^2 - 1)$, $[R_B, \tau_d] = (1 - \tau_d^2)R_A$, and $[R_B, R_A] = (\tau_d^2 - 1)\tau_d^{-1}$. We choose the Bloch representation where $\psi_{n,q}^{e,h}(z)$ are simultaneously eigenfunctions of τ_d and H with eigenvalues e^{iqd} and $\epsilon_{n,q}^{e,h}$, respectively. Here e and h refer to conduction and valence states and n is a subband index, while q is the superlattice wave vector along the growth (z) axis. For $q=0$ and $q=\pi/d$, which corresponds to standing and not-traveling Bloch waves, all these commutators vanish and we can choose the Bloch envelope functions F_ν as eigenfunctions of R_A and R_B . The eigenvalues are ± 1 , corresponding to wave functions which are even or odd with respect to O_A, O_B . The relation

$$R_B R_A F_{\nu q} = e^{iqd} F_{\nu q} \quad (1)$$

shows that the parity with respect to the centers of one type of layer must be the same at $q=0$ and $q=\pi/d$, and that the parity with respect to the centers of the other type of layer must be opposite at $q=0$ and $q=\pi/d$ (see Table I).

To calculate the interband-matrix element, we make use of the translational invariance of the effective Hamiltonian in the layers planes:

$$\psi_{nq_1}^{e,h}(z, \vec{r}_1) = \sum_{\nu} \frac{1}{\sqrt{S}} C_{\nu nq_1}^{e,h} U_\nu(z, \vec{r}_1) e^{i\vec{k}_1 \cdot \vec{r}_1} f_{\nu nq_1}^{e,h}(z). \quad (2)$$

In (2), \vec{r}_1 and \vec{k}_1 are two-dimensional vectors in the layer planes of area S . $C_{\nu nq_1}^{e,h}$ are normalization coefficients and $f_{\nu nq_1}^{e,h}$ the z -dependent part of the envelope function which varies slowly at the scale of d_0 (but not of d). For an electromagnetic wave propagating parallel to the SL axis, the interband-matrix element M_{nm} becomes proportional to a sum of $\rho_{\nu\nu}$ optical matrix elements between the quickly varying functions U_ν multiplied by the over-

TABLE I. Truth table of the parity statements.

		R_A	R_B		R_A	R_B
$q=0$	$(R_B R_A = +1)$	+1	+1	or	-1	-1
$q=\pi/d$	$(R_B R_A = -1)$	± 1	∓ 1		∓ 1	± 1

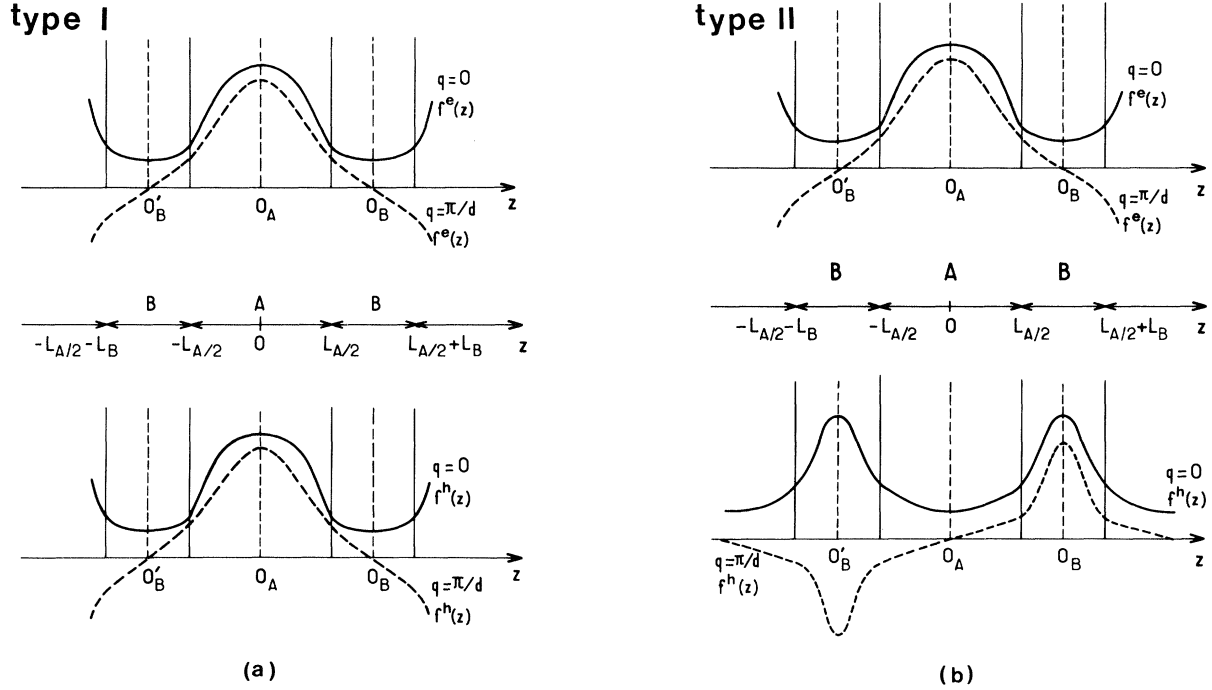


FIG. 2. Schematic envelope functions for conduction and valence ground subbands at $q=0$ (solid lines) and $q=\pi/d$ (dashed lines) in type-I (a) and type-II (b) SL's.

lap integrals between the slowly varying envelopes

$$M_{nm}(q, \vec{k}_\perp) = \sum_{\nu, \nu'} C_{\nu n q \vec{k}_\perp}^{*e} C_{\nu' m q \vec{k}_\perp}^h \rho_{\nu \nu'} \times \int_{-d/2}^{+d/2} dz f_{\nu n q \vec{k}_\perp}^{*e}(z) f_{\nu' m q \vec{k}_\perp}^h(z), \quad (3)$$

where we have made use of the wave-vector conservation for interband transitions in any perfect solid. For interband transitions between the few low-lying subbands associated with the host conduction and valence bands, the summation in Eq. (3) can be truncated to the few band edges which contribute significantly to (2). Let us for simplicity assume that the two hosts conduction and valence bands are well energy separated, or equivalently that the host bands are parabolic. Then in Eq. (3) only ν (identically equal to conduction) (S -like) and ν' (identically equal to valence) (P -like) come into play. For type-I systems, we assume that f_{nq}^e and f_{mq}^h both retain the same symmetry with respect to O_A at both $q=0$ and $q=\pi/d$. Then if the transition is parity allowed at $q=0$ (which is the case if $n+m$ is even) it will remain parity allowed at $q=\pi/d$, as illustrated in Fig. 2(a). On the other hand, in a type-II SL f_{nq}^e (respectively, f_{mq}^h) is expected to retain the same parity with respect to O_A (respectively, O_B) at both $q=0$ and π/d . If the transition is parity allowed at $q=0$ [say, that f_{nq}^e and f_{mq}^h are even with respect to O_A as in Fig. 2(b)], then this transition becomes forbidden at $q=\pi/d$ because in the integral in Eq. (3) f_{nq}^e has remained even with respect to O_A , whereas f_{mq}^h has become odd with respect to the same point. Note, however, that this conclusion

does not hold if nonparabolicity effects become dramatic, which occurs in semimetallic InAs/GaSb SL's (Refs. 6 and 9) when the first conduction and light-hole subbands anticross. In this case, the complete calculation Eq. (3) has to be performed.

III. EXPLICIT CALCULATIONS: TIGHT-BINDING ANALYSIS OF THE ENVELOPE FUNCTIONS

In most cases of actual interest, the SL subbands widths are smaller than the energy separation between the various levels of the isolated quantum wells from which they originate. It is then reasonable to use a tight-binding description of the envelope functions $f_{\nu n q \vec{k}_\perp}(z)$. The superlattice potential is written as a sum of atomlike potentials:

$$V_c(z) = \sum_{n=-\infty}^{+\infty} v_c(z - nd),$$

$$V_v(z) = \sum_{n=-\infty}^{\infty} v_v(z - nd - \sigma d/2),$$

$$v_c(x) = -V_c \text{ if } |x| < L_A/2 \text{ and } 0 \text{ elsewhere,} \quad (4)$$

$$v_v(x - \sigma d/2) = V_v$$

if $|x - \sigma d/2| < [L_A + (1 - \sigma)L_B]/2$ and 0 elsewhere, for conduction- and valence-band edges, respectively. V_c and V_v are positive quantities. The index σ is equal to 0 (1) in type-I (type-II) superlattices. We again restrict ourselves to the parabolic case. The isolated quantum-well problems are assumed to be solved: Let $\phi_{nk_1}^e(z - jd)$ and

$\phi_{mk_1}^h(z - jd - \sigma d/2)$ be the eigenfunctions of the bound states of the conduction- and valence-isolated quantum wells at the site labeled j , with the eigenenergies $\lambda_{nk_1}^e$, $\lambda_{mk_1}^h$. Since the Hamiltonian of the quantum-well problem commutes with the reflection with respect to the center of the well, the ϕ_n functions have the parity $(-1)^n$ with respect to this point. Generally speaking, the k_1 dependence of the ϕ 's functions is weak and, for the sake of simplicity, we will ignore it in the following. In the simplest tight-binding scheme, the ϕ_n 's functions centered at different sites are orthogonal and the transfer integrals

$$\langle \phi_n(z - id) | v(z - id) | \phi_n(z - jd) \rangle$$

vanish unless $j = i \pm 1$. The SL envelope functions are written as

$$\begin{aligned} f_{nq}^e(z) &= \frac{1}{\sqrt{N}} \sum_{p=-\infty}^{\infty} \phi_n^e(z - pd) e^{iqpd}, \\ f_{mq}^h(z) &= \frac{1}{\sqrt{N}} \sum_{p=-\infty}^{\infty} \phi_n^h(z - pd - \sigma d/2) e^{iqpd}, \end{aligned} \quad (5)$$

where N is the (large) number of SL unit cells in the crystal. The overlap integral $\langle f_{nq}^e | f_{mq}^h \rangle$ is equal to

$$P_{nm}(q) = \sum_{p=-\infty}^{\infty} e^{iqpd} \mu_{nm}(p), \quad (6)$$

where

$$\mu_{nm}(p) = \int_{-\infty}^{+\infty} dz \phi_n^e(z) \phi_m^h(z - pd - \sigma d/2). \quad (7)$$

A. Type-I systems

For these systems $\sigma = 0$ and with the use of the symmetry properties of the ϕ 's, Eq. (6) can be rewritten as

$$P_{nm}(q) = \mu_{nm}(0) + \begin{cases} 2 \sum_{p=1}^{\infty} \cos(qpd) \mu_{nm}(p), & n+m \text{ even}, \\ 2i \sum_{p=1}^{\infty} \sin(qpd) \mu_{nm}(p), & n+m \text{ odd}. \end{cases} \quad (8)$$

(9)

$\mu_{nm}(0)$ is nonvanishing only if $m+n$ is even, the diagonal term $m=n$ being much more intense than the off-diagonal ones. For $p \neq 0$, $\mu_{nm}(p)$ has no selection rule but is exponentially small as compared to $\mu_{nm}(0)$. To a very good approximation $P_{nm}(q)$ is independent of q and equal to $\mu_{nm}(0)$. In Eqs. (8) and (9) we have recovered the exact properties found in II: If at $q=0$ the transition is parity allowed ($m+n$ even), it remains allowed at $q=\pi/d$. Symmetrically, if it is forbidden at $q=0$ ($m+n$ odd), it remains forbidden at $q=\pi/d$.

B. Type-II systems

Here $\sigma = 1$ and we may rewrite Eq. (6) as

$$P_{nm}(q) = \sum_{p=0}^{\infty} e^{iqpd} [1 + (-1)^{n+m} e^{-i(2p+1)qd}] \mu_{nm}(p). \quad (10)$$

None of the μ 's vanishes and all are exponentially small, being nonzero only through the leakage of the ϕ 's functions outside the wells where they are centered. As in (a) we recover explicitly the general property found in Sec. II. If the transition is parity allowed at $q=0$ ($m+n$ even), then it becomes parity forbidden at $q=\pi/d$. Reciprocally, if $m+n$ is odd, the transition is allowed at $q=\pi/d$ and forbidden at $q=0$. In contrast with type-I systems, $P_{nm}(q)$ depends strongly on q . To the lowest order, we have

$$P_{nm}(q) = \begin{cases} 2\mu_{nm}(0) e^{-iqd/2} \cos(qd/2), & m+n \text{ even}, \\ 2i\mu_{nm}(0) e^{-iqd/2} \sin(qd/2), & m+n \text{ odd}. \end{cases} \quad (11)$$

$$(12)$$

IV. ABSORPTION AND EMISSION SPECTRA IN SUPERLATTICES

The q dependence of the interband-matrix element found in type-II SL, as well as its absence in type-I SL, drastically affects the interband absorption and emission line shapes. Besides, the orders of magnitude of the $\mu_{nm}(0)$'s are so different in the two types of SL's that a measurement of the absorption coefficient appears to be sufficient to determine quite unambiguously which type of SL is under investigation.

A. Absorption

For a transition between given valence $|vmq\rangle$ and conduction $|cnq\rangle$ states, the absorption coefficient reads

$$\begin{aligned} K_{nm}(q) &= \frac{2\pi e^2}{m_0^2 \epsilon_0 \epsilon_r^{1/2} c \omega \Omega} |\langle U_c | P | U_v \rangle|^2 \\ &\times \sum_{k_1} |P_{nm}(q)|^2 \delta(\epsilon_{nk_1q}^c - \epsilon_{mk_1q}^h - \hbar\omega), \end{aligned} \quad (13)$$

where m_0 is the free-electron mass, ϵ_r the SL relative dielectric constant, $\hbar\omega$ the photon energy, and Ω the volume of the sample. P is the component of electron momentum along the polarization axis. A twofold spin degeneracy has been taken into account. The energy differences between conduction and valence states appearing in the δ function in Eq. (13) can be written as

$$\begin{aligned} \epsilon_{nk_1q}^e - \epsilon_{mk_1q}^h &= \epsilon_A(1 - \sigma) + (\epsilon_B - V_c)\sigma \\ &+ \lambda_{n,k_1=0}^e + \lambda_{m,k_1=0}^h \\ &+ 2(t_n^e - t_m^h) \cos(qd) + \hbar^2 k_1^2 / 2M_{nm}^\perp, \end{aligned} \quad (14)$$

where M_{nm}^\perp is the electron-hole reduced mass, possibly n, m dependent, for the motion in the layers planes. ϵ_A (ϵ_B) is the A (B) material band gap and t_n^e and t_m^h are the transfer integrals

$$t_n^{e(h)} = \langle \phi_n^{e(h)}(z) | v_{c(v)}(z) | \phi_n^{e(h)}(z-d) \rangle, \quad (15)$$

where t_n^e is negative (positive) when n is odd (even) whereas t_m^h is positive (negative) when m is odd (even). To be specific let us consider a SL built from III-V or II-VI

compounds. For these materials we have

$$E_p = \frac{2}{m_0} |\langle S | P_x | X \rangle|^2 \sim 23 \text{ eV}. \quad (16)$$

A transition from heavy-hole to conduction subbands involves $\frac{1}{2} |\langle S | P_x | X \rangle|^2$, while light-hole to conduction subbands involves $\frac{1}{6} |\langle S | P_x | X \rangle|^2$. The absorption coefficient associated with a heavy-hole to conduction subbands transition is equal to

$$K_{nm}^{hh \rightarrow e}(\omega) = \frac{e^2}{4\epsilon_0 d} \frac{M_{nm}^{\perp}}{m_0} \frac{E_p}{\epsilon_r^{1/2} c \omega \hbar^2} \times \int_0^1 dx \left| P_{nm} \left[\frac{\pi x}{d} \right] \right|^2 Y(\hbar\omega - E_g(x)), \quad (17)$$

where

$$E_g(x) = \epsilon_A(1 - \sigma) + (\epsilon_B - V_c)\sigma + \lambda_{n,k_1=0}^e + \lambda_{m,k_1=0}^h + 2(t_n^e - t_m^h) \cos(\pi x). \quad (18)$$

For light-hole to conduction subbands transitions, this expression should simply be divided by 3. Retaining only the lower terms in the Fourier expansion of the overlap integral $P_{nm}(q)$ [Eq. (6)], the integral in Eq. (17) is easily evaluated. We express the photon energy in dimensionless units

$$\hbar\omega = \epsilon_A(1 + \sigma) + (\epsilon_B - V_c)\sigma + \lambda_{n,k_1=0}^e + \lambda_{m,k_1=0}^h + 2(t_n^e - t_m^h)(1 - 2\xi). \quad (19)$$

For odd-to-odd transitions, for example, the absorption coefficient (17) is found to be equal to

$$K_{nm}^I(\omega) = \frac{C}{\pi} \left| \mu_{nm}^I(0) \right|^2 \begin{cases} 0, & \xi < 0 \\ \arccos(1 - 2\xi), & 0 \leq \xi \leq 1 \\ \pi, & \xi > 1, \end{cases} \quad (20)$$

$$K_{nm}^{II}(\omega) = \frac{2C}{\pi} \left| \mu_{nm}^{II}(0) \right|^2 \times \begin{cases} 0, & \xi < 0 \\ \arccos(1 - 2\xi) + 2\sqrt{\xi(1 - \xi)}, & 0 \leq \xi \leq 1 \\ \pi, & \xi > 1, \end{cases} \quad (21)$$

for type-I and type-II superlattices, respectively. C is the prefactor of the integral in Eq. (17). In both types of SL's the absorption coefficient becomes flat (if we neglect the slight ω dependence of C) once ($\xi > 1$) the photon energy exceeds the threshold energy ($\xi = 0$) plus the sum of the bandwidths $4|t_n^e| + 4|t_m^h|$. The plateau is characteristic of a two-dimensional behavior in the layer planes, hence the proportionality of K to the transverse mass M_{nm}^{\perp} . Close to the onset of the absorption ($\xi \rightarrow 0^+$), the superlattice behaves like a three-dimensional, anisotropic material characterized by reduced masses M_{nm}^{\perp} and M_{nm}^{\parallel} perpendic-

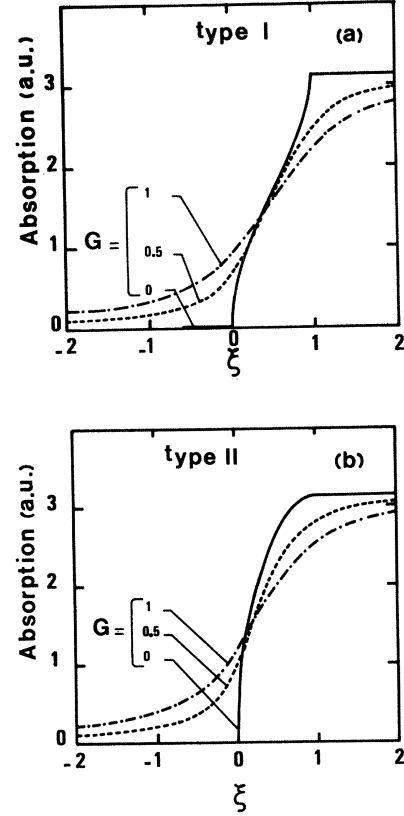


FIG. 3. Absorption line shapes in type-I (a) and type-II (b) SL's. ξ is the reduced photon energy and G the phenomenological damping parameter, as defined in the text.

ular and parallel to the superlattices axis, respectively, with

$$M_{nm}^{\parallel} = \hbar^2 / 2d^2 (-t_n^e + t_m^h). \quad (22)$$

In type-I SL's the transition to a two-dimensional behavior at $\xi = 1$ is eye marked by a Van Hove singularity as the optical absorption is proportional to the joint density of states of the two bands [Fig. 3(a)]. This singularity is blurred in type-II SL's by the q dependence of the overlap integral which vanishes at the zone boundary [Fig. 3(b)]. Note, however, that the absorption line shape is not necessarily a decisive criterion for establishing which type of superlattice is under investigation because of the unavoidable existence of damping mechanisms. A rough, qualitative, description of these effects on the absorption line shapes is obtained by replacing in Eq. (17) the step function $Y(x)$ by $\frac{1}{2} + \pi^{-1} \arctan(x/\Gamma)$, where Γ is the broadening energy. The influence of G , the dimensionless damping parameter defined as

$$G = (\Gamma/2) (-t_n^e + t_m^h), \quad (23)$$

is shown on Fig. 3(a) and 3(b). The type-I and type-II absorption line shapes become very similar for $G \geq 0.5$. Since Γ is at best 2–3 meV, SL bandwidths of at least 5–10 meV are required to separate the broadening in-

duced from the superlattice-induced contributions to the absorption tails which are always observed below the two-dimensional-like plateaux.

However, a clear-cut difference still exists between type-I and type-II SL's absorption, which is linked to an "atomiclike" property: we have shown in Sec. III that $\mu_{nm}^I(0)$ is much larger than $\mu_{nm}^{II}(0)$ because of the spatial separation of the carriers which occurs in type-II systems. Assume that all the physical parameters (but the μ 's) are the same in a type-I and a type-II SL. Far enough from the threshold, the absorption coefficients are flat and we have

$$K_{nm}^{II}(\omega)/K_{nm}^I(\omega) = 2 |\mu_{nm}^{II}(0)|^2 / |\mu_{nm}^I(0)|^2.$$

The μ 's can be easily evaluated from the solution of the isolated quantum-well problems. For instance, for $n=m=1$ and the parameters of the GaAs/Al_{0.2}Ga_{0.8}As system: $m_c=0.067m_0$, $m_{hh}=0.47m_0$, $V_c=0.2$ eV, $V_v=0.035$ eV, $L_A=102$ Å, and $L_B=92$ Å, we have found $|\mu_{11}^I|^2 \sim 1$ while in a type-II system with the same band parameters, we get $|\mu_{11}^{II}|^2 \sim 1.7 \times 10^{-2}$. The prefactor C/π in Eq. (20) is equal to 2.8×10^3 cm⁻¹ with $\epsilon_r=13.1$ and $\hbar\omega=1.6$ eV. For a type-II SL the absorption coefficient is then very small ($\lesssim 10^2$ cm⁻¹) and requires rather thick samples to be revealed. The absorption coefficient in a type-I SL is much larger. Still it is smaller than the absorption coefficient for bulk-A material. For multiquantum well (MQW) structures in the thick well limit, for instance, we have

$$K_{11}^I(\xi=1)/K_{\text{bulk}}(\xi=1) = L_A/L_A + L_B. \quad (25)$$

Miller *et al.*¹² have recently measured the absorption coefficient of GaAs-Ga(Al)As MQW's. The absorption coefficient in MQW's is distinctly smaller than the bulk GaAs one, in qualitative agreement with the previous discussion. In semiconducting InAs-GaSb type-II SL's Chang *et al.*⁸ have found absorption coefficients of the order of few 10^2 cm⁻¹ at the onset of the superlattice band-gap absorption. Our calculations are in qualitative agreement with these experiments.

B. Emission

With the same parameters as used in the previous sections, and assuming nondegenerate distributions for electrons and holes (room-temperature band-to-band recombination), the energy emission spectrum is given by

$$\Lambda(\omega) = \alpha \omega^2 e^{-\xi/\theta} K_{11}^{I(II)}(\xi), \quad (26)$$

where θ is the dimensionless thermal energy

$$\theta = kT/4(t_1^{hh} - t_1^e). \quad (27)$$

The details of the SL band parameters are included in the α coefficient, which may slightly depend on the energy in case of strong nonparabolicity. Figures 4(a) and 4(b) show the dimensionless emission spectra $\Lambda(\omega)/\alpha\omega^2$ for type-I and type-II SL's, respectively, and for two values of θ , $\theta=0.5$ and 1. It is clear on these figures that for a given temperature, the maximum of the emission line occurs at a lower energy in a type-II SL than in a type-I SL, even

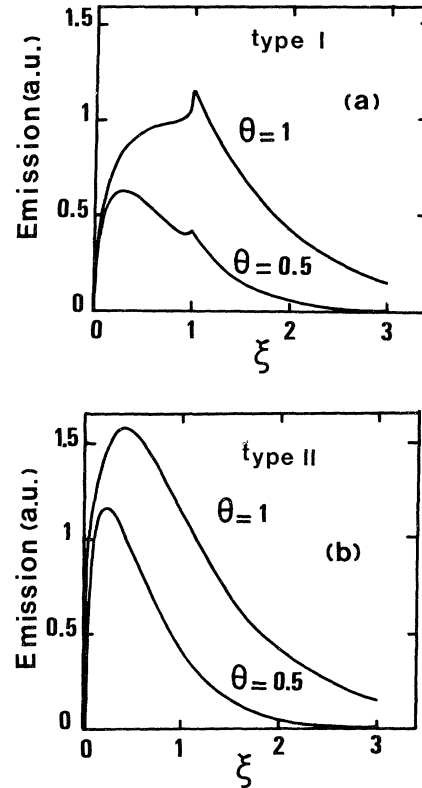


FIG. 4. Reduced band-to-band emission line shapes for type-I (a) and type-II (b) SL's. θ is the reduced thermal energy as defined in the text.

though characterized by the same bandwidth. Because of the Van Hove singularity at $q=\pi/d$, the type-I emission spectra exhibit a spike at $\xi=1$. Such a spike is blurred by the q dependence of the optical matrix element in type-II systems. Hence the determination of effective electron temperature, SL band parameters, etc., obtained from a fit of the band-to-band recombination line shape is crucially dependent upon a correct description of the q dependence of the interband-matrix element and therefore of the SL wave functions.

V. CONCLUSION

We have investigated theoretically the interband optical properties of superlattices. The superlattice electronic states have been described by the envelope function approximation. The q dependence of the optical matrix element is negligible for type-I SL's while it is crucial for type-II systems. We have given a quantitative discussion of the absorption coefficient which should be relevant to the determination of the nature (type I or type II) of a given SL (Ref. 10) as well as to the discussion of the relative strengths of magneto-optical transitions in SL's.⁹ However, in high-quality type-I superlattices, excitonic effects have been observed,¹¹ which considerably influence the absorption lineshapes.

Finally, the parity selection rules derived in Secs. II and

III exist only because we have neglected the noncentrosymmetric nature of the III-V (or II-VI) unit cells as well as the effect associated with layer edges. These two approximations may seem severe at first glance. However, the quasi-Ge model is known to work very well in bulk II-V and II-VI materials (it is indeed extremely hard to measure the strength of the inversion asymmetry constant in bulk III-V materials). As far as edge effects are concerned (i.e., that the terminating planes are made of different atoms in the right-hand and left-hand sides of a

given layer), they should be small for thick (i.e., actual) layers. In fact, the only transitions seen in absorption experiments performed on isolated QW structures¹¹ fulfill a parity selection rule (Δn even) as if indeed the parity operator R_A were commuting with the effective Hamiltonian.

ACKNOWLEDGMENT

We gladly thank Dr. F. Laloé for fruitful discussions.

-
- ¹G. A. Sai-Halasz, L. Esaki, and W. A. Harrison, *Phys. Rev. B* **18**, 2812 (1978).
²J. N. Schulman and Y. C. Chang, *Phys. Rev. B* **24**, 4445 (1981).
³G. C. Osbourn, *J. Appl. Phys.* **53**, 1586 (1982).
⁴S. R. White and L. J. Sham, *Phys. Rev. Lett.* **27**, 879 (1981).
⁵T. Ando and S. Mori, *Surf. Sci.* **113**, 124 (1982).
⁶G. Bastard, *Phys. Rev. B* **24**, 5693 (1981); **25**, 7584 (1982).
⁷M. Altarelli, Proceedings of the 16th International Conference on the Physics of Semiconductors, Montpellier, 1982 [*Physica* **117&118B**, 747 (1983)].
⁸L. L. Chang, G. A. Sai-Halasz, L. Esaki, and R. L. Aggarwal, *J. Vac. Sci. Technol.* **19**, 589 (1981).
⁹J. C. Maan, Y. Guldner, J. P. Vieren, P. Voisin, M. Voos, L. L. Chang, and L. Esaki, *Solid State Commun.* **39**, 683 (1981).
¹⁰P. Voisin, G. Bastard, M. Voos, E. E. Mendez, C. A. Chang, L. L. Chang, and L. Esaki, Proceedings of the International Conference on Metastable and Modulated Semiconductor Structures, Pasadena, 1982 [*J. Vac. Sci. Technol. B* **1**, 409 (1983)].
¹¹R. Dingle, in *Festkörperprobleme XV (Advances in Solid State Physics)*, edited by H. J. Queisser (Pergamon-Vieweg, Braunschweig, 1975), p. 21.
¹²D. A. B. Miller, D. S. Chemla, D. J. Eilenberger, P. W. Smith, A. C. Grossard, and W. T. Tsang, *Appl. Phys. Lett.* **41**, 679 (1982).